Article

Protective Effects of *Oenothera Biennis* Against Hydrogen Peroxide-Induced Oxidative Stress and Cell Death in Skin Keratinocytes

Seung Young Lee [1], Chul Hwan Kim [1], Buyng Su Hwang [1], Kyung-Min Choi [1], In-Jun Yang [2], Gi-Young Kim [3], Yung Hyun Choi [4], Cheol Park [5,*] and Jin-Woo Jeong [1,*]

[1] Nakdonggang National Institute of Biological Resources, 137, Donam 2-gil, Sangju-si, Gyeongsangbuk-do 37242, Republic of Korea ; nplsy001@nnibr.re.kr (S.Y.L.); kchul1204@nnibr.re.kr (C.H.K.); hwang1531@nnibr.re.kr (B.S.H.); kyungmc69@nnibr.re.kr (K.-M.C.)

[2] Department of Physiology, College of Oriental Medicine, Dongguk University, Gyeongju 780-714, Republic of Korea.; injuny@gmail.com (I.-J.Y.)

[3] Laboratory of Immunobiology, Department of Marine Life Sciences, Jeju National University, Jeju 63243, Republic of Korea; immunkim@jejunu.ac.kr (G.-Y.K.)

[4] Department of Plant System Science, College of Natural Science, Chung-Ang University, Anseong 17546, Republic of Korea; choiyh@deu.ac.kr (Y.H.C.)

[5] Division of Basic Sciences, College of Liberal Studies, Dong-eui University, Busan, 47340, Republic of Korea.

* Correspondence: parkch@deu.ac.kr (C.P.); jwjeong@nnibr.re.kr (J.-W.J.); Tel.: +82-51-890-1530 (C.P.); Tel.: +82-54-530-0884 (J.-W.J.)

Abstract: Background: *Oenothera biennis* (evening primrose) produces bioactive substances with a diverse range of pharmacological functions. However, it is currently unknown whether extract prepared from the aerial parts of *O. biennis* (APOB) can protect the skin against oxidative stress. To investigate the protective effects of APOB against oxidative stress-induced damage in human skin keratinocytes (HaCaT) and elucidate the underlying mechanisms. Methods: We pretreated HaCaT cells with various concentrations of APOB or the antioxidant N-acetyl-L-cysteine before applying H_2O_2. We then compared the cell viability, intracellular reactive oxygen species (ROS) production, and DNA and mitochondrial damage between pretreated and untreated control cells using a range of assays, flow cytometry, and Western blot analysis and also examined the reducing power and DPPH free radical-scavenging activity of APOB. Results: APOB pretreatment significantly increased cell viability, effectively attenuated H_2O_2-induced comet tail formation, and inhibited H_2O_2-induced phosphorylation of the histone γH2AX, as well as the number of apoptotic bodies and Annexin V-positive cells. APOB was found to have a high reducing power and DPPH radical-scavenging activity and also exhibited scavenging activity against intracellular ROS accumulation and restored the loss of mitochondrial membrane potential caused by H_2O_2. APOB pretreatment almost totally reversed the enhanced cleavage of caspase-3, the degradation of poly (ADP-ribose)-polymerase (PARP), DNA fragmentation that usually occurs in the presence of H_2O_2 and increased the levels of heme oxygenase-1 (HO-1), a potent antioxidant enzyme that is associated with the induction of nuclear factor-erythroid 2-related factor 2 (Nrf2). Conclusions: APOB can protect HaCaT cells from H_2O_2-induced DNA damage and cell death by blocking cellular damage related to oxidative stress via a mechanism that affects ROS elimination and by activating the Nrf2/HO-1 signaling pathway.

Keywords: *Oenothera biennis;* Evening primrose; Oxidative stress; Cell death; Nrf2/HO-1

1. Introduction

Living organisms produce reactive oxygen species (ROS) as byproducts of the normal cellular metabolism of oxygen [1]. These substances are required for normal physiological processes, acting as cellular messengers in redox signaling. However, the uncontrolled release of ROS can induce

 doi:10.20944/preprints202009.0194.v1

oxidative DNA damage. Human skin is a barrier to the external environment, making keratinocytes highly susceptible to oxidative injury that may cause ROS production. The resulting DNA damage contributes to the initiation of cellular apoptosis, eventually leading to disruption of the epithelial structure of the skin and resulting in the pathogenesis of a number of human skin disorders [2,3]. The development of safer and more effective antioxidants for skin protection remains an important research goal. Our bodies possess several defense mechanisms to maintain ROS at low physiological levels and counteract this oxidative stress; the Nrf2/HO-1 signaling pathway is an important mediator of cellular injury in response to oxidative stress [4]. Ergothioneine is known to exhibit dermato-protective effects against ultraviolet A injury by inducing Nrf2/ARE-mediated antioxidant genes in human keratinocytes [5], and Nrf2 silencing significantly reduces the expression of many antioxidant enzymes, including HO-1, and sensitizes immortalized non-tumorigenic human skin keratinocytes (HaCaT) to acute cytotoxicity [6].

Herbs were once primarily used as traditional medicines to treat various kinds of diseases but are now used in pharmacology, cosmetics, perfumery, nutraceuticals, beverages, and dying industries. The biennial herbaceous plant *Oenothera biennis* L. (evening primrose), is widely distributed throughout eastern and central North America and Asia [7], has several beneficial effects on human health [8,9], and its seeds and their extracts have recently been found to have antioxidant and free radical-scavenging activities [10]. However, the chemical composition and bioactivities of extracts prepared from the aerial parts of *O. biennis* (APOB) and the molecular mechanisms involved remain unclear.

We investigated the protective effects of APOB extract against H_2O_2-induced ROS generation, oxidative damage, and cell death in HaCaT keratinocytes.

2. Materials and Methods

2.1. *Preparation of APOB Extract*

Aerial parts of *O. biennis* were air-dried at room temperature and ground to powder using a mechanical grinder. Approximately 100 g of the powder was then added to 2 L ethanol and stirred continuously at 100 rpm for 24 h at room temperature. The resulting extract was filtered and the solvent was removed by rotary vacuum evaporation (N-1000S; EYELA, Tokyo, Japan). The extract was then dissolved in dimethyl sulfoxide (DMSO; Sigma-Aldrich Chemical Co., St. Louis, MO, USA) to obtain a 100 mg/mL stock solution and stored at 4°C. This solution was diluted to the desired concentration with physiological saline prior to use.

2.2. *Chromatographic Analysis of APOB*

APOB sample was dissolved in 10 mg/mL methanol; its phytochemical composition was analyzed using high-performance liquid chromatography (HPLC) with an Agilent 1200 series HPLC instrument (Agilent Technologies, San Jose, CA, USA) and an Agilent ZORBAX Extend-C18 column (250 × 4.6 mm). The column was operated in gradient mode with a mixture of 0.1% formic acid in water (A) and acetonitrile (B) as solvents (eluent B: 5%–100% in 55 min), a flow rate of 1 ml/min, and an injection volume of 20 µL. The chromatograms were recorded at 320 nm, and each peak was in the UV/visible spectrum (200–400 nm).

2.3. *Liquid Chromatography-Tandem Mass Spectroscopy (LC-MS/MS) Analysis of APOB*

An APOB sample was dissolved in 0.1 mg/ml methanol (100 ppm) and analyzed by LC-MS/MS using an AB Sciex QTrap® 4500 system (Sciex, USA) coupled to an ultra-performance liquid chromatography system (Shimadzu, Japan) with photodiode array and mass detectors. A Luna Omega Polar C18 column (2.1 × 150 mm; 1.6 µm; Phenomenex, Torrance, CA, USA) was used as the stationary phase, and 0.1% formic acid in water (A) and 0.1% formic acid in acetonitrile (B) were used as the mobile phase (gradient mode; eluent B: 5%–95% in 16 min), with a flow rate of 0.3 mL/min and an injection volume of 2 µL. Components were identified at 320 nm. MS with an electrospray ionization (ESI) source in negative mode was used with the following optimized parameters: curtain

 doi:10.20944/preprints202009.0194.v1

gas, 35 °C; temperature, 500 °C for gas source 1 and 40 °C for gas source 2; ion spray voltage, 4.5 kV for negative ion mode; delisting potential, 135 V; scan range, m/z 200–800.

2.4. *Isolation of Peak 4*

A dried APOB sample (600 g) was extracted with ethanol at room temperature and filtered. The filtrate was evaporated under reduced pressure to give the extract (80 g), which was suspended in water (500 ml) and successively partitioned with n-hexane, $CHCl_3$, ethyl acetate (EtOAc), and n-butanol, yielding 10, 5, 7, and 25 g, respectively. The EtOAc layer (2.0 g) was separated on an RP-C18 silica gel column with 30–100% methyl alcohol (MeOH) to yield nine fractions (E1–E9). Fraction E6 (100 mg) was chromatographed using a Sephadex LH-20 column (80% MeOH) and an RP-C18 preparative HPLC column (50% MeOH) to yield peak 4 (2 mg). The structure of peak 4 was identified by comparing the proton nuclear magnetic resonance (1H-NMR) and MS spectral data with literature [11].

2.5. *Cell Culture and Cell Viability Assay*

The HaCaT cell line was obtained from the American Type Culture Collection (Manassas, MD, USA) and cultured in Roswell Park Memorial Institute (RPMI) 1640 medium (Gibco BRL, Grand Island, NY, USA) containing 10% heat-inactivated fetal bovine serum (Gibco BRL), streptomycin (100 μg/ml), and penicillin (100 units/ml). Cells were maintained at 37 °C and 5% CO_2 in an incubator.

For the cell viability assay, HaCaT cells were seeded in 6-well plates at 3×10^5 cells/ml and cultured for 24 h before being treated with various concentrations of APOB (0–100 μg/mL) or the antioxidant N-acetyl-L-cysteine (NAC; 10 mM) for 24 h in the presence or absence of H_2O_2. The cells were then incubated with 3-[4,5-dimethylthiazo l-2-yl]-2,5diphenyltetrazolium bromide (MTT) solution (0.5 mg/mL) and incubated for 3 h at 37 °C in the dark; the medium was removed and formazan precipitate was dissolved in DMSO. The absorbance of the formazan product was measured at 540 nm using a Cytation-3 microplate reader (BioTek, Shoreline, WA, USA).

2.6. *Reducing Power and Scavenging Activity of APOB*

The reducing power of APOB was determined using the method described [12]. APOB extracts (0–100 μg/mL) were dissolved in phosphate buffer (0.1 M, pH 6.6) and added to 1% potassium ferricyanide (50 mL, 0.5 g). Each mixture was incubated at 50 °C for 30 min; 10% trichloroacetic acid (50 mL, 5 g) was added. The supernatant (100 μL) was mixed with distilled water (100 μL) and 0.1% ferric chloride (10 mL, 0.01 g), and the absorbance was measured at 700 nm with a Cytation-3 microplate reader. The result was converted to 100 μg/mL of ascorbic acid equivalent based on the standard curve for ascorbic acid.

The 2,2-diphenyl-1-picrylhydrazyl (DPPH) radical-scavenging activity was determined using the method described [13]. A 100 μL aliquot of the diluted APOB extracts (0–100 μg/mL) was added to a methanolic solution (100 μL) of DPPH radical (final concentration, 0.2 mM). The mixture was shaken vigorously and left to stand at room temperature for 30 min in the dark. The absorbance of the resulting solution was then measured spectrophotometrically at 517 nm. The tests were run in duplicate, and all samples were analyzed in triplicate and averaged.

2.7. *Intracellular ROS Production*

An oxidation-sensitive dye 2′,7′-dichlorodihydrofluorescein diacetate (DCF-DA; Molecular Probes, Eugene, OR, USA) was used to determine the formation of intracellular ROS. Briefly, the cells were harvested, washed twice with phosphate-buffered saline (PBS), and resuspended in 10 μM DCF-DA at 37 °C for 30 min in the dark. The cells were then washed with PBS and their FL-1 fluorescence was measured with a flow cytometer (FACS Calibur; Becton Dickinson, San Jose, CA, USA).

2.8. *Comet Assay*

 doi:10.20944/preprints202009.0194.v1

Treated cells were washed with PBS, mixed with 0.5% low melting agarose (LMA) at 37 °C, and mounted on slides pre-coated with 1% normal melting agarose. After solidification of the agarose, the slides were covered with another layer of 0.5% LMA and immersed in lysis buffer [2.5 M NaCl, 500 mM Na-ethylenediaminetetraacetic acid (EDTA; Sigma-Aldrich Chemical Co.), 1 M Tris buffer, 1% sodium lauryl sarcosine, and 1% Triton X-100] for 1 h at 4 °C. The slides were then transferred into an unwinding buffer for 20 min for DNA unwinding and placed in an electrophoresis tank containing 300 mM NaOH and 1 mM Na-EDTA (pH 13). An electrical field was applied (300 mA, 25 V) for 20 min at 25 °C to draw the negatively charged DNA toward the anode. The slides were washed three times in a neutralizing buffer (0.4 M Tris, pH 7.5) for 5 min at 25 °C, stained with 20 μg/mL propidium iodide (PI; Sigma-Aldrich Chemical Co.), and examined under a fluorescence microscope (Carl Zeiss, Oberkochen, Germany).

2.9. *Protein Extraction and Western Blot Analysis*

The HaCaT cells were gently lysed with lysis buffer [20 mM sucrose, 1 mM EDTA, 20 μM Tris-Cl (pH 7.2), 1 mM dithiothreitol (DTT), 10 mM KCl, 1.5 mM $MgCl_2$, 5 μg/ml aprotinin] for 30 min. The supernatants were collected and the protein concentrations were quantified using a Bio-Rad Protein Assay Kit (Bio-Rad Laboratories, Hercules, CA, USA). For Western blot analysis, equal amounts of proteins were subjected to electrophoresis on sodium dodecyl sulfate-polyacrylamide gels and then electro-transferred to a polyvinylidene fluoride membrane (Schleicher & Schuell, Keene, NH, USA). The resulting blots were probed with the desired antibodies, incubated with the diluted enzyme-linked secondary antibodies, and visualized by enhanced chemiluminescence, following the recommended procedure (Amersham Corp., Arlington Heights, IL, USA).

2.10. *Mitochondrial Membrane Potential (MMP) Assay*

The MMP of intact cells was measured by DNA flow cytometry with the rationmetric, dual-emission fluorescent dye JC-1, which is internalized and concentrated by respiring mitochondria. JC-1 remains a monomer at low MMPs (FL-1, green fluorescence; 527 nm) and forms aggregates at high MMPs (FL-2, red fluorescence; 590 nm) according to the recommended procedure (Calbiochem). The treated cells were trypsinized, and the cell pellets were resuspended in PBS and incubated with 10 μM JC-1 for 20 min at 37 °C; they were washed once with cold PBS, suspended, and analyzed using flow cytometry.

2.11. *Cell Death*

A fluorescein-conjugated Annexin V (Annexin V-FITC) staining assay kit (BD Biosciences, San Jose, CA, USA) was used to quantitatively assess the level of induced cell apoptosis. Briefly, the treated cells were washed with PBS, stained with 5 μL Annexin V-FITC and 5 μL, and incubated for 15 min at room temperature in the dark. The degree of apoptosis was then quantified as the percentage of Annexin V-positive and PI-negative (Annexin V^+/PI^-) cells using a flow cytometer.

2.12. *Statistical Analysis*

All experiments were replicated in three independent experiments. All data were expressed as the mean ± SD and analyzed using the GraphPad Prism software (version 5.03; GraphPad Software, Inc., La Jolla, CA, USA). ANOVA with Bonferroni multiple comparison test was used to confirm significant differences among the group means. A value of $p < 0.05$ was considered to represent a statistically significant difference.

3. Results

3.1. *Chemical Characterization of APOB*

Preprints (www.preprints.org) | NOT PEER-REVIEWED | Posted: 9 September 2020 doi:10.20944/preprints202009.0194.v1

We used HPLC and LC-MS/MS with ESI to characterize the APOB extract. Four major peaks were identified in the HPLC profile of the APOB extract (Figure 1). Peaks 1, 2, and 3 were tentatively identified as 3-caffeoylquinic acid, ellagic acid, and quercetin 3-O-glucuronide, respectively, by comparing the UV spectra, mass data, and fragmentation patterns with published values [14]. The ESI-MS spectrum of peak 4 exhibited an [M−H]− ion at m/z 433 and a fragment at m/z 301 due to the loss of a pentoside unit. The 1H-NMR spectrum of peak 4 showed signals that were characteristic of quercetin (δ 7.75, br s; δ 7.60, br d, J = 8.3 Hz; δ 6.90, d, J = 8.3 Hz; δ 6.42, br s; and δ 6.22, br s) and a pentoside unit (δ 5.50, br s; δ 4.35, br d, J = 1.2 Hz; and δ 3.95–3.50, m); peak 4 was tentatively identified as quercetin 3-O-pentoside (arabinofuranoside) based on published values [11].

(A)

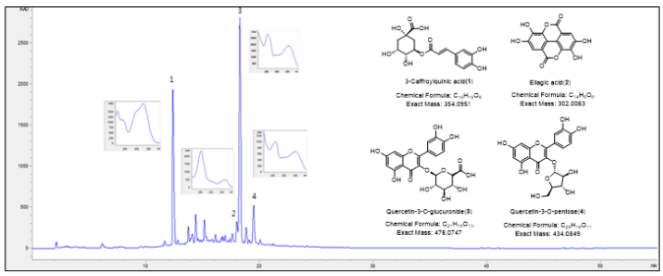

(B)

Peak	R_t (min)	UV (nm)	$[M-H]^-$ (m/z)	Fragmentation	Tentative compound of Identification
1	12.38	327	353	191, 173	3-Caffeoylquinic acid
2	17.99	254, 368	301	258, 253	Ellagic acid
3	18.25	256, 356	477	301	Quercetin 3-O-glucuronide
4	19.48	258, 354	433	301	Quercetin 3-O-pentose(arabinofuranoside)

Figure 1. Fingerprint analysis of APOB. (A) HPLC analysis of the four reference compounds and APOB. (B) LC-MS/MS analysis of the major compounds in APOB ethanol extract.

3.2. *Effects of APOB on H_2O_2-Induced Cytotoxicity*

The MTT assay indicated that APOB extract did not induce any cytotoxic effects at concentrations up to 60 μg/mL but gradually reduced cell viability at concentrations of 80 μg/mL or more (Figure 2A). We used ≤ 60 μg/mL APOB to examine its protective effects against H_2O_2-induced cytotoxicity. MTT assays revealed that treatment with 0.5 mM H_2O_2 significantly reduced cell viability. APOB pretreatment effectively protected cells from this effect in a concentration-dependent manner, as did NAC pretreatment (Figure 2B).

3.3. *Reducing Power and DPPH Radical-Scavenging Activity of APOB*

The presence of antioxidants causes the Fe^{3+}/ferric cyanide complex to be reduced to the ferrous form, the concentration of which can be monitored by measuring the formation of Perl's Prussian blue at 700 nm. We assessed the ability of APOB to reduce Fe^{3+} to Fe^{2+} using the method [15], using ascorbic acid as a positive control. APOB exhibited a dose-dependent reducing power across the measured concentrations (0, 20, 40, and 60 μg/mL), with 60 μg/mL APOB having the highest reducing power (Figure 2C). We also investigated the DPPH radical-scavenging assay is a quick, reliable, and reproducible method for determining the in vitro antioxidant activity of pure compounds and plant extracts [18] and has been used widely in model systems to investigate the scavenging activities of natural compounds. The antioxidant activity of APOB increased with increasing concentrations (Figure 2D).

Preprints (www.preprints.org) | NOT PEER-REVIEWED | Posted: 9 September 2020 doi:10.20944/preprints202009.0194.v1

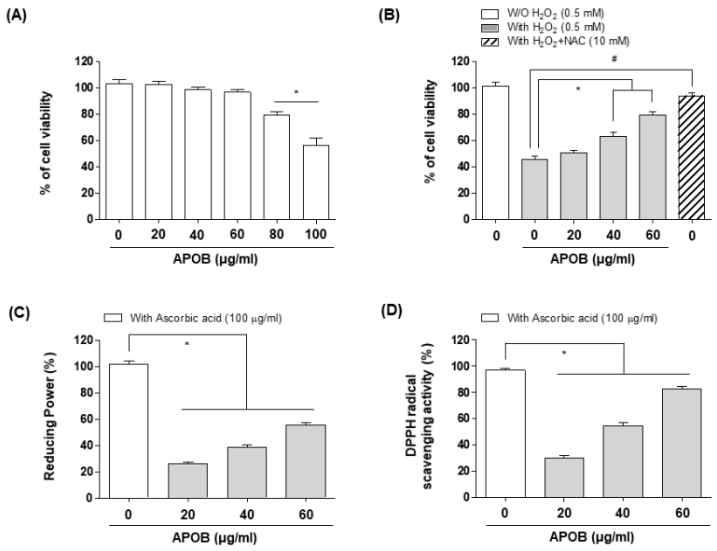

Figure 2. Protective effects of APOB against H2O2-induced cytotoxicity and its antioxidant activity in HaCaT cells. (A and B) MTT assays of cell viability in cells treated with APOB alone (A) or pretreated with or without APOB or NAC and then induced with H2O2 (B). (C) Reducing power and (D) DPPH scavenging activity of APOB. Data are expressed as the means ± SD of three independent experiments (ANOVA: * $p < 0.05$ vs. control group).

3.4. *Effect of APOB on H_2O_2-Induced ROS Generation*

We used the ROS-sensitive fluorescent dye DCF-DA to investigate whether APOB prevents H_2O_2-induced ROS generation. HaCaT cells that had been exposed to H_2O_2 for 30 min showed a significant increase in the accumulation of intracellular ROS, whereas this induction was substantially inhibited by APOB or NAC pretreatment (Figure 3). APOB treatment alone did not increase ROS generation.

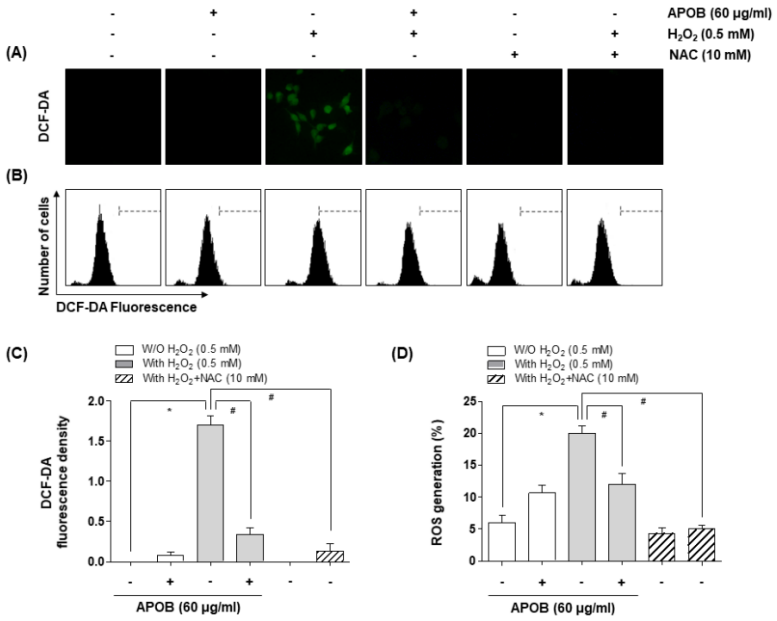

Figure 3. Effects of APOB on H2O2-induced ROS generation in HaCaT cells. ROS generation was measured by (A and C) fluorescence microscopy and (B and D) flow cytometry. Each point represents the mean ± SD of three independent experiments (ANOVA: *$p < 0.05$ vs. untreated control; #$p < 0.05$ vs. H2O2-treated cells).

Preprints (www.preprints.org) | NOT PEER-REVIEWED | Posted: 9 September 2020 doi:10.20944/preprints202009.0194.v1

3.5. *Effect of APOB on H_2O_2-Induced DNA Damage*

The comet assay, measuring both single and double-strand breaks [16], showed that H_2O_2 treatment increased the amount of DNA in the tail (tail moment) and the distance of DNA migration (tail length); APOB pretreatment significantly reduced both effects (Figure 4). Immunoblotting revealed that H_2O_2 exposure increased histone γH2AX phosphorylation on serine 139, a marker of DNA double-strand breaks [17]; APOB pretreatment effectively inhibited this adverse effect (Figure 5).

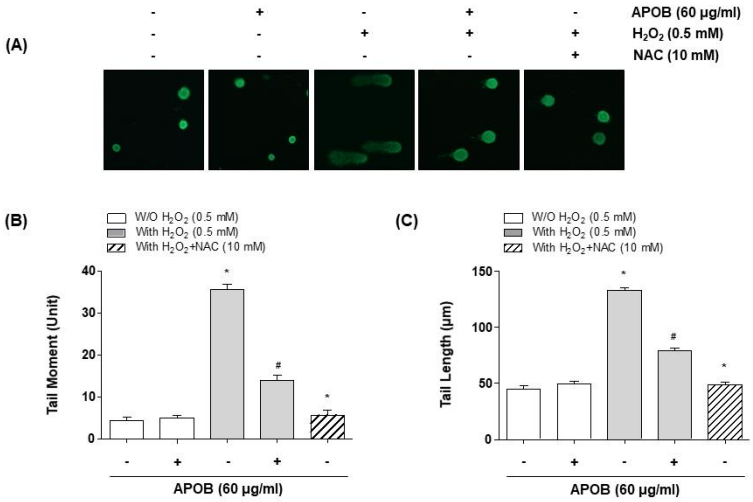

Figure 4. Effects of APOB on H2O2-induced DNA damage in HaCaT cells (comet assay). (A) Representative pictures of the comets taken using a fluorescence microscope (original magnification, 200×). (B and C) The average tail moments and tail lengths of at least 100 cells per experimental point (ANOVA: *p < 0.05 vs. untreated control group; #p < 0.05 vs. H2O2-treated group).

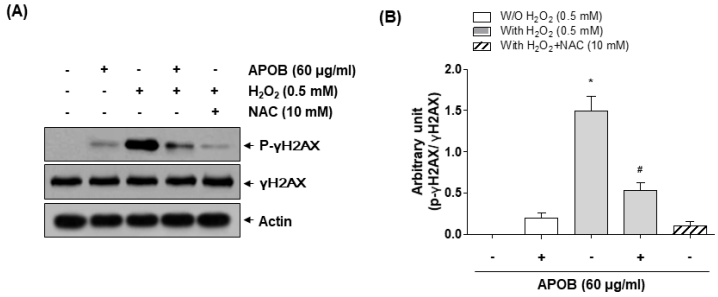

Figure 5. Effects of APOB on H2O2-induced phosphorylation of γH2AX in HaCaT cells. (A) Western blot analysis of the cell contents using specific antibodies against γH2AX and p-γH2AX and actin as an internal control. (B) Relative expression of p-γH2AX compared with γH2AX (ANOVA: *p < 0.05 vs. untreated control group; #p < 0.05 vs. H2O2-treated group).

3.6. *Effect of APOB on H_2O_2-Induced Mitochondrial Dysfunction*

Bacause mitochondrial dysfunction due to ROS attack is thought to contribute to cell death [18], we assessed depolarization of the mitochondrial membrane and opening of the mitochondrial permeability transition pore (mPTP) (sensitive indicators of mitochondrial function). H_2O_2-treated cells exhibited mitochondrial depolarization and an mPTP opening, as indicated by an increase in FL-1 (JC-1 monomers) compared with control and APOB-treated cells (Figure 6).

Preprints (www.preprints.org) | NOT PEER-REVIEWED | Posted: 9 September 2020 doi:10.20944/preprints202009.0194.v1

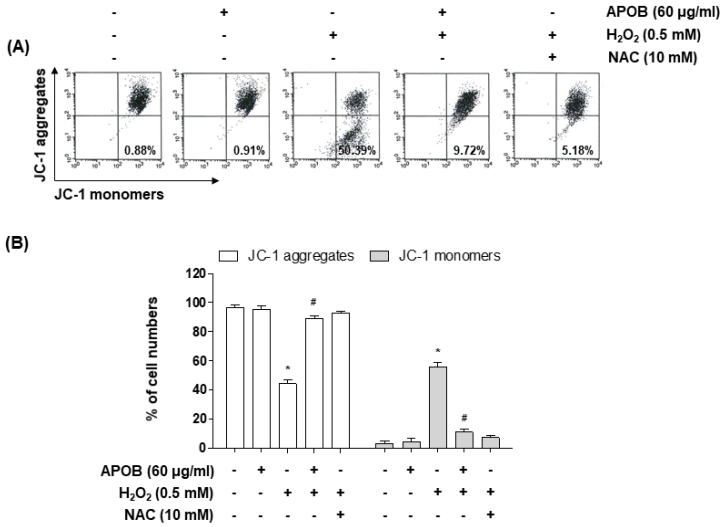

Figure 6. Effect of APOB on H2O2-induced mitochondrial dysfunction in HaCaT cells. (A) Flow cytometry analysis of MMP. (B) Amounts of JC-1 aggregates and monomers. Each point represents the mean ± SD of three independent experiments (ANOVA: *$p < 0.05$ vs. untreated control; #$p < 0.05$ vs. H2O2-treated cells).

3.7. *Effect of APOB on H_2O_2-Induced Cell Death*

We next H_2O_2 treatment significantly increased the number of condensed or blebbing nuclei, the population of Annexin V^+/PI^- (apoptotic) cells, and the formation of DNA laddering, whereas APOB pretreatment markedly reduced these effects (Figure 7).

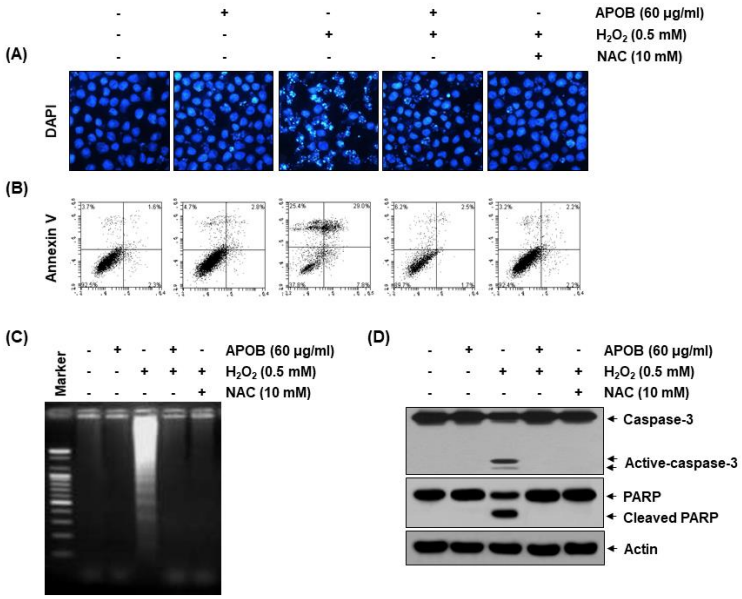

Figure 7. Effects of APOB on H2O2-induced chromatin condensation, Annexin V production, DNA fragmentation, caspase-3 cleavage, and PARP degradation in HaCaT cells. (A) Observation of DAPI-stained nuclei under a fluorescence microscope (original magnification, 400×). (B) Percentage of apoptotic cells in each treatment group. (C) Level of DNA fragmentation. (D) Western blot analysis of the cell contents using specific antibodies against caspase-3 and PARP and actin as an internal control.

 doi:10.20944/preprints202009.0194.v1

3.8. *Effects of APOB on the Expressions of Nrf2 and HO-1*

Activation of the Nrf2/HO-1 signaling pathway plays an important role in antioxidant activity [19]; we investigated the effect of APOB on the expressions of Nrf2 and its regulator HO-1. Immunoblotting showed that APOB treatment increased the expressions of Nrf2 and HO-1 in a dose-dependent manner but decreased Keap1 expression (Figure 8A). APOB treatment also increased phosphorylation at serine 40, required for the activation and stabilization of Nrf2. Although Nrf2 expression and phosphorylation were similar between H_2O_2-treated cells and untreated control cells, they were markedly elevated in cells that were co-treated with APOB and H_2O_2 (Figure 8B), and co-treated cells also had much higher levels of HO-1 expression and a reduced Keap1 expression compared with cells treated with APOB alone.

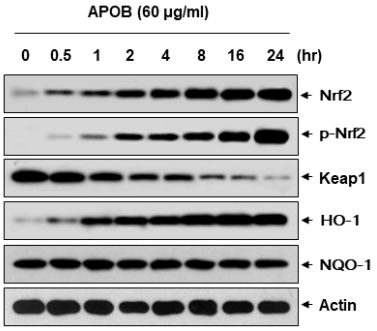

Figure 8. Induction of Nrf2 and HO-1 expression by APOB in HaCaT cells. The proteins were visualized using the detection system, with actin as an internal control for the total cellular and nuclear proteins.

4. Discussion

We explored APOB protective efects against H_2O_2 damage in HaCaT keratinocytes and defined the cytoprotective mechanism involved. APOB significantly rescued the viability of H_2O_2-treated HaCaT cells and exhibited a high reducing power and scavenging activity. We demonstrated that this protection against oxidative stress was mediated by the inhibition of DNA damage, mitochondrial dysfunction, ROS generation, and caspase-3 activation and was also associated with activation of the Nrf2/HO-1 signaling pathway.

Oxidative stress is an abnormal phenomenon where the production of free radicals exceeds the antioxidant capacity. Extremely elevated levels of ROS can destroy cytoprotective defense mechanisms of neutralizing antioxidants, accelerating skin aging and the development of various skin diseases [20], causing a range of irreversible base modifications and DNA strand breaks resulting in DNA damage [3]. Elevated levels of ROS also induce mitochondrial dysfunction, resulting in a decrease in MMP and the release of mitochondrial apoptotic factors into the cytoplasm, causing the activation of caspase-9 and caspase-3 [2]. Caspase-3 activation is involved in the cleavage or degradation of various important proteins that are involved in apoptosis, including PARP, and so plays a primary role in triggering the cascade of events that lead to the apoptosis pathway [21]. ROS-generation prevention by antioxidant agents is considered a possible strategy for reducing oxidative damage to the skin [22].

APOB significantly protected HaCaT cells against H_2O_2-induced growth inhibition and DNA damage; hence, it may enhance DNA repair. APOB could effectively restore the H_2O_2-induced loss of MMP to the basal level and prevent caspase-3 activation and PARP cleavage by H_2O_2 in HaCaT cells, indicating that its ability to attenuate oxidative stress partly depends on the inhibition of mitochondrial-related apoptosis. Additionally, APOB pretreatment substantially inhibited elevated ROS accumulation in H_2O_2-exposed cells, indicating its free radical-scavenging activity and protective properties.

There is growing evidence that the Nrf2-mediated signaling pathway is essential in protecting human skin fibroblasts against oxidative stress [4]. Under basal conditions, Nrf2-dependent transcription is suppressed by Keap1, facilitating Nrf2 degradation through ubiquitin-mediated proteasomal degradation [23]. Upon modification of specific thiols by oxidative insult, Keap1 triggers the dissociation of Nrf2 from the Nrf2-Keap1 complex, allowing Nrf2 to translocate from the cytoplasm to the nucleus, where it subsequently activates AREs present in the promoter regions of an array of genes [6,19]. The status of Nrf2 and its inhibitory protein Keap-1 determines Nrf2-mediated ARE activity [4]. Additionally, Nrf2 phosphorylation also leads to its nuclear export [24]. We investigated whether the Nrf2 pathway contributes to the protective effects of APOB against H_2O_2-induced oxidative stress in HaCaT cells.

Nrf2 expression and phosphorylation were significantly higher in cells that had been co-treated with H_2O_2 and APOB compared with those that were treated with APOB alone, whereas Keap1 expression was lower. Moreover, HO-1 expression was significantly upregulated in H_2O_2 and APOB co-treated cells, indicating that APOB could activate the Nrf2/HO-1 antioxidant pathway. Although further experiments are needed to determine the mechanisms of inhibition of ROS production and activation of the Nrf2/HO-1 axis, these results show that the Nrf2/HO-1 signaling pathway may contribute to the protective ability of APOB against H_2O_2-mediated oxidative stress. APOB may represent an important natural skin protective agent with promising applications in dermatological clinical research.

5. Conclusions

APOB is a potent antioxidant that can prevent oxidative DNA damage and reduce ROS generation and activation of the mitochondria-mediated apoptotic pathway in H_2O_2-treated HaCaT keratinocytes. This protective action involves Nrf2 activation and upregulation of the expression of its downstream antioxidant gene HO-1. APOB may be of therapeutic value in the prevention and treatment of various human skin diseases associated with oxidative stress. Further studies are required, particularly using human systems, to determine the cellular uptake, distribution, and long-term effects of APOB on the skin.

Author Contributions: C.P. and J.-W.J. conceptualized the study, supervised experiments, supported the study, and wrote the paper. S.Y.L. helped design and perform experiments. C.H.K., B.S.H. and K.-M.C. helped with various experiments. I.-J.Y., G.-Y.K. and Y.H.C. shared reagents and helped in editing the paper. All authors have read and agreed to the published version of the manuscript.

Funding: This work was supported by a grant from the Nakdonggang National Institute of Biological Resources (NNIBR), funded by the Ministry of Environment (MOE) of the Republic of Korea (NNIBR2020002106).

Conflicts of Interest: The authors declare no conflict of interest.

References

1. Crack, P.J.; Taylor, J.M. Reactive oxygen species and the modulation of stroke. *Free Radic. Biol. Med.* **2005**, 38, 1433–1444.
2. Cadet, J.; Douki, T.; Ravanat, J.L. Oxidatively generated damage to cellular DNA by UVB and UVA radiation. *Photochem. Photobiol.* **2015**, 91, 140–155.
3. Katiyar, S.K. Dietary proanthocyanidins inhibit UV radiation-induced skin tumor development through functional activation of the immune system. *Mol. Nutr. Food Res.* **2016**, 60, 1374–1382.
4. Loboda, A.; Damulewicz, M.; Pyza, E.; Jozkowicz, A.; Dulak, J. Role of Nrf2/HO-1 system in development, oxidative stress response and diseases: An evolutionarily conserved mechanism. *Cell. Mol. Life Sci.* **2016**, 73, 3221–3247.
5. Hseu, Y.C.; Lo, H.W.; Korivi, M.; Tsai, Y.C.; Tang, M.J.; Yang, H.L. Dermato-protective properties of ergothioneine through induction of Nrf2/ARE-mediated antioxidant genes in UVA-irradiated human keratinocytes. *Free Radic. Biol. Med.* **2015**, 86, 102–117.

6. Zhao, R.; Hou, Y.; Zhang, Q.; Woods, C.G.; Xue, P.; Fu, J.; Yarborough, K.; Guan, D.; Andersen, M.E.; Pi, J. Cross-regulations among NRFs and KEAP1 and effects of their silencing on arsenic-induced antioxidant response and cytotoxicity in human keratinocytes. *Environ. Health Perspect*. **2012**, 120, 583–589.
7. Mihulka, S.; Pysek, P. Invasion history of Oenothera congeners in Europe: A comparative study of spreading rates in the last 200 years. *J. Biogeogr*. **2001**, 28, 597–609.
8. Kim, T.S.; Shin, K.; Jeon, J.H.; Choi, E.K.; Choi, Y.; Lee, S.P.; Lee, Y.B.; Kim, Y.B. Comparative analysis of anti-*Helicobacter pylori* activities of FEMY-R7 composed of Laminaria japonica and *Oenothera biennis* extracts in mice and humans. *Lab. Anim. Res*. **2015**, 31, 7–12.
9. Gorlach, S.; Wagner, W.; Podsedek, A.; Sosnowska, D.; Dastych, J.; Koziolkiewicz, M. Polyphenols from evening primrose (*Oenothera paradoxa*) defatted seeds induce apoptosis in human colon cancer caco–2 cells. *J. Agric. Food Chem.* **2011**, 59, 6985-6997.
10. Peschel, W.; Dieckmann, W.; Sonnenschein, M.; Plescher. A. High antioxidant potential of pressing residues from evening primrose in comparison to other oilseed cakes and plant antioxidants. *Ind. Crops Prod*. **2007**, 25, 44–54.
11. da Silva Sá, F.A.; de Paula, J.A.M.; Dos Santos, P.A.; de Almeida Ribeiro Oliveira, L.; de Almeida Ribeiro Oliveira, G.; Lião, L.M.; de Paula, J.R.; do Rosário Rodrigues Silva, M. Phytochemical analysis and antimicrobial activity of *Myrcia tomentosa* (Aubl.) DC. Leaves. *Molecules* **2017**, 22, E1100.
12. Yen, G.C.; Chen, H.Y. Antioxidant activity of various tea extracts in relation to their antimutagenicity. *J. Agric. Food Chem.* **1995**, 46, 849–854.
13. Cheel, J.; Theoduloz, C.; Rodriguez, J.; Schmeda-Hirschmann, G. Free radical scavengers and antioxidants from lemongrass (*Cymbopogon citratus* (DC.) Stapf.). *J. Agric. Food Chem.* **2005**, 53, 2511–2517.
14. Timoszuk, M.; Bielawska, K.; Skrzydlewska, E. Evening Primrose (*Oenothera biennis*) biological activity dependent on chemical composition. *Antioxidants* **2018**, 7, E108.
15. Ferreira, I.C.F.R.; Baptista, P.; Vilas-Boas, M.; Barros, L. Free-radical scavenging capacity and reducing power of wild edible mushrooms from northeast Portugal: Individual cap and stipe activity. *Food Chem.* **2007**, 100, 1511–1516.
16. Azqueta, A.; Slyskova, J.; Langie, S.A.; O'Neill Gaivão, I.; Collins, A. Comet assay to measure DNA repair: Approach and applications. *Front. Genet*. **2014**, 5, 288.
17. Rogakou, E.P.; Pilch, D.R.; Orr, A.H.; Ivanova, V.S.; Bonner, W.M. DNA double-stranded breaks induce histone H2AX phosphorylation on serine 139. *J. Biol. Chem*. **1998**, 273, 5858–5868.
18. Cha, M.Y.; Kim, D.K.; Mook-Jung, I. The role of mitochondrial DNA mutation on neurodegenerative diseases. *Exp. Mol. Med*. **2015**, 47, E150.
19. Murakami, S.; Motohashi, H. Roles of Nrf2 in cell proliferation and differentiation. *Free Radic. Biol. Med.* **2015**, 88, 168–178.
20. Masaki, H. Role of antioxidants in the skin: Anti–aging effects. *J. Dermatol. Sci.* **2010**, 58, 85–90.
21. Hensley, P.; Mishra, M.; Kyprianou, N. Targeting caspases in cancer therapeutics. *Biol. Chem.* **2013**, 394, 831–843.
22. Tundis, R.; Loizzo, M.R.; Bonesi, M.; Menichini, F. Potential role of natural compounds against skin aging. *Curr. Med. Chem.* **2015**, 22, 1515–1538.
23. O'Connell, M.A.; Hayes, J.D. The Keap1/Nrf2 pathway in health and disease: From the bench to the clinic. *Biochem. Soc. Trans*. **2015**, 43, 687–689.
24. Kaspar, J.W.; Jaiswal, A.K. Tyrosine phosphorylation controls nuclear export of Fyn, allowing Nrf2 activation of cytoprotective gene expression. *FASEB J.* **2011**, 25, 1076–1087.
25.